The ISME Journal (2014) 8, 295–308

www.nature.com/ismej

ORIGINAL ARTICLE

High-fat diet alters gut microbiota physiology in mice

Hannelore Daniel[1], Amin Moghaddas Gholami[2,13], David Berry[3,13], Charles Desmarchelier[1,13], Hannes Hahne[2,13], Gunnar Loh[4], Stanislas Mondot[5,6], Patricia Lepage[5], Michael Rothballer[7], Alesia Walker[8], Christoph Böhm[3], Mareike Wenning[9], Michael Wagner[3], Michael Blaut[4], Philippe Schmitt-Kopplin[8], Bernhard Kuster[2,10], Dirk Haller[11] and Thomas Clavel[11,12]

[1]*Molecular Nutrition Unit, ZIEL-Research Center for Nutrition and Food Sciences, Technische Universität München, Freising-Weihenstephan, Germany;* [2]*Proteomics and Bioanalytics, Technische Universität München, Freising-Weihenstephan, Germany;* [3]*Division of Microbial Ecology, Department of Microbiology and Ecosystem Science, Faculty of Life Sciences, University of Vienna, Vienna, Austria;* [4]*Department of Gastrointestinal Microbiology, German Institute of Human Nutrition Potsdam-Rehbrücke (DIfE), Nuthetal, Germany;* [5]*INRA/AgroParisTech, Micalis UMR1319, Jouy-en-Josas, France;* [6]*CSIRO Livestock Industries, Queensland Bioscience Precinct, St Lucia, Australia;* [7]*Research Unit Plant-Microbe Interactions, Helmholtz Zentrum München, Neuherberg, Germany;* [8]*Analytical BioGeoChemistry, Helmoltz Zentrum München, Neuherberg, Germany; Chair of Analytical Food Chemistry, Technische Universität München, Freising-Weihenstephan, Germany;* [9]*Microbiology, ZIEL-Research Center for Nutrition and Food Sciences, Technische Universität München, Freising-Weihenstephan, Germany;* [10]*Center for Integrated Protein Science Munich, Germany;* [11]*Chair of Nutrition and Immunology, Technische Universität München, Freising-Weihenstephan, Germany and* [12]*Junior Research Group Intestinal Microbiome, ZIEL-Research Center for Nutrition and Food Sciences, Technische Universität München, Freising-Weihenstephan, Germany*

The intestinal microbiota is known to regulate host energy homeostasis and can be influenced by high-calorie diets. However, changes affecting the ecosystem at the functional level are still not well characterized. We measured shifts in cecal bacterial communities in mice fed a carbohydrate or high-fat (HF) diet for 12 weeks at the level of the following: (i) diversity and taxa distribution by high-throughput 16S ribosomal RNA gene sequencing; (ii) bulk and single-cell chemical composition by Fourier-transform infrared- (FT-IR) and Raman micro-spectroscopy and (iii) metaproteome and metabolome via high-resolution mass spectrometry. High-fat diet caused shifts in the diversity of dominant gut bacteria and altered the proportion of *Ruminococcaceae* (decrease) and *Rikenellaceae* (increase). FT-IR spectroscopy revealed that the impact of the diet on cecal chemical fingerprints is greater than the impact of microbiota composition. Diet-driven changes in biochemical fingerprints of members of the *Bacteroidales* and *Lachnospiraceae* were also observed at the level of single cells, indicating that there were distinct differences in cellular composition of dominant phylotypes under different diets. Metaproteome and metabolome analyses based on the occurrence of 1760 bacterial proteins and 86 annotated metabolites revealed distinct HF diet-specific profiles. Alteration of hormonal and anti-microbial networks, bile acid and bilirubin metabolism and shifts towards amino acid and simple sugars metabolism were observed. We conclude that a HF diet markedly affects the gut bacterial ecosystem at the functional level.
The ISME Journal (2014) **8,** 295–308; doi:10.1038/ismej.2013.155; published online 12 September 2013
Subject Category: Microbe-microbe and microbe-host interactions
Keywords: diet-induced obesity; high-fat diet; intestinal microbiota; metabolomics; metaproteome; spectroscopy

Introduction

Over the last century, the field of clinical microbiology has been driven by the study of pathogens (Raoult *et al.,* 2004), but recently, the importance of commensal microorganisms that colonize various body habitats has been brought to light (Lepage *et al.,* 2013). In particular, the gut microbial ecosystem has emerged as an important factor regulating host health and the onset of chronic diseases such as inflammatory bowel diseases, allergies and obesity (Blaut and Clavel, 2007; Delzenne and Cani, 2011; Kau *et al.,* 2011; Hörmannsperger *et al.,* 2012).

A proof of the causative role of gut microbes in influencing host metabolism was provided by the

Correspondence: T Clavel, Junior Research Group Intestinal Microbiome, ZIEL-Research Center for Nutrition and Food Sciences, Technische Universität München, Gregor-Mendel-Strasse 2, 85350 Freising-Weihenstephan, Germany.
E-mail: thomas.clavel@tum.de
[13]These authors contributed equally to the work.
Received 13 June 2013; accepted 4 August 2013; published online 12 September 2013

observation that transfer of gut microbiota from obese donor mice to germfree mice fed a standard diet promoted adiposity (Backhed *et al.,* 2004; Turnbaugh *et al.,* 2009). Nonetheless, the quantitative contribution of the gut microbiota to host energy balance remains elusive. Jumpertz *et al.,* (2011), recently proposed that an increased energy harvest of *ca.* 150 kcal is associated with an increase of 20% in the sequence occurrence of *Firmicutes* and a corresponding decrease in the *Bacteroidetes* in humans, although the impact of high inter-individual differences in the percentage of energy lost in stools have been discussed (Heymsfield and Pietrobelli, 2011). Driven by the popularization of DNA sequencing-based approaches, many studies have described changes in gut bacterial diversity and composition after ingestion of high-energy diets (Cani *et al.,* 2008; Turnbaugh *et al.,* 2008; Fleissner *et al.,* 2010). However, the consequences of such changes in bacterial diversity on the function of the ecosystem are still unclear. Major advances in the assessment of microbial gene occurrence by large-scale metagenomic sequencing have shed light on the genomic potential of the gut microbiota and have indicated possible changes in microbial activity related to diet and metabolic disorders (Turnbaugh *et al.,* 2006; Qin *et al.,* 2012). Nonetheless, direct proofs of changes in activity and function of the ecosystem in response to dietary challenge are urgently required. Therefore, in the present work, we used a combination of high-resolution spectroscopic and mass spectrometric techniques for in-depth characterization of the cecal ecosystem in mice. We thereby provide novel insights into biochemical alterations of the gut microbiota in response to a high-fat (HF) diet.

Materials and methods

Animals and samples

All procedures were conducted according to the German guidelines for animal care and approved by the state ethics committee (ref. no. 209.1/211-2531-41/03). The design of mouse trials has been described elsewhere (Desmarchelier *et al.,* 2012, 2013). Details are given in the Supplementary Methods. Male C57BL/6NCrl mice ($n=6$ per group) were fed an experimental carbohydrate (CARB) or HF diet for 12 weeks (Table 1). The data presented in this paper were obtained in the course of four feeding trials with exactly the same design (Supplementary Figure S1). In trial 1–3, after cecal weight determination, the content was divided into two portions that were snap frozen in liquid nitrogen. In trial 4, cecal contents were used in their entirety in order to obtain sufficient starting material (metaproteome via LC-MS/MS, $n=4$; metabolome via Fourier-transform ion cyclotron resonance mass spectrometry (FT-ICR-MS), $n=3$).

Table 1 Diet composition

	CARB	*HF*
GE (MJ kg^{-1})	18.0	25.2
ME (MJ kg^{-1})	15.0	21.4
% carbohydrate	66.0	21.0
% protein	23.0	19.0
% fat	11.0	60.0
Crude protein	20.8	24.1
Crude fat	4.2	34.0
Crude fiber	5.0	6.0
Crude ash	5.6	6.1
Starch	48.8	1.1
Sugar	10.8	8.2
Dextrins	—	15.6
Sodium	0.2	0.2
Casein	24.0	27.7
Corn starch	49.8	—
Maltodextrin	—	15.8
Glucose	10.0	—
Sucrose	—	8.0
Cellulose	5.0	6.0
Vitamin premix	1.0	1.2
Mineral/trace elements	6.0	6.1
L-cystine	—	0.4
Choline chloride	0.2	0.3
Salt (NaCl)	—	0.1
Butylhydroxytoluol	—	<0.1
Beef tallow (premier jus)	—	31.0
Soybean oil	4.0	3.0

Abbreviations: CARB, carbohydrate; GE, gross energy; HF, high-fat; ME, metabolizable energy calculated with the Atwater factors. Nutrient contents are given in percentages (g 100 g^{-1}). All experimental diets were ordered from Ssniff GmbH (Soest, Germany): CARB, cat. no. E15000-04; HF, E15741-34. The composition of the standard laboratory chow diet (Ssniff GmbH, cat. no. V1534) used for 2 weeks prior to dietary treatment was: dry matter, 87.7; crude protein, 19.0; crude fat, 3.3; crude fiber, 4.9; crude ash, 6.4; starch, 36.5; sugar/dextrins, 4.7; GE, 16.3; ME, 12.8; % carbohydrate, 58; % protein, 33; % fat, 9.

Experiments with germfree mice were performed as explained in the Supplementary Methods.

High-throughput sequencing

Cecal samples were analyzed by sequencing the V4 region (233 bp) of 16S ribosomal RNA (rRNA) genes in paired-end modus using the MiSeq system (Illumina, San Diego, CA, USA). Detailed instructions are given in the Supplementary Methods. The first 10 and last 20 nucleotides of all reads were trimmed using the NGS-QC toolkit (New Dehli, India) (Patel and Jain, 2012) to avoid GC bias and non-random base composition as well as low sequence quality at 3′-end. Reads were assembled using Pandaseq with a minimum overlap of 35 bp (Masella *et al.,* 2012). Sequences were further analyzed using the open source software package QIIME (Boulder, CO, USA) (Caporaso *et al.,* 2010) and the Ribosomal Database Project (East Lansing, MI, USA) (Cole *et al.,* 2003). Filtering parameters were as follows: minimum Phred score, 20; minimum number of high-quality calls, 0.65; maximum number of consecutive low-quality base calls, 5. Operational taxonomic units were picked against the Greengenes

database (Berkeley, CA, USA) at a threshold of 97% similarity and those occurring in less than three mice and with a total number of less than three sequences were excluded from the analysis.

Fourier-transform infrared spectroscopy
In Fourier-transform infrared (FT-IR) spectroscopy, samples are excited by an infrared beam and transmitted light is recorded, resulting in spectra showing at which wavelengths samples absorb light, depending on the nature of covalent bounds. Thereby, FT-IR spectroscopy gives information on the overall biochemical composition of microbial cells, and can be a useful tool for the identification of pure cultures (Wenning *et al.,* 2006). Saline solution (0.9% NaCl in water) was used for sample preparation by centrifugation to obtain cecal microbial pellets (Supplementary Methods). Re-suspended pellets in saline solution (referred to as cecal suspensions hereon) were analyzed by transmission using a TENSOR 27 spectrometer coupled with a HTS-XT high-throughput device (Bruker Optics, Ettlingen, Germany). The spectrum of each sample was computed from 32 scans. Spectral similarities were assessed by hierarchical cluster analysis using the OPUS software version 6.5 (Bruker).

Confocal Raman microspectroscopy
Fluorescence *in situ* hybridization (FISH) was used to identify target populations for Raman microspectroscopic analysis, which utilizes the principle of Raman scattering to chemically fingerprint individual microbial cells (Huang *et al.,* 2007). The probes used in the present study were Bac-0303 5′-CCA ATG TGG GGG ACC TT-3′ (Manz *et al.,* 1996) and Erec-0482 5′-CGC GGC ATT GCT CGT TCA-3′ (Franks *et al.,* 1998) (Thermo Fisher Scientific, Vienna, Austria). Cecal samples that had been fixed in 4% paraformaldehyde were hybridized on aluminum slides using a previously described hybridization protocol (Berry *et al.,* 2012). Spectra of cells from target populations were acquired using a LabRAM HR800 confocal Raman microscope (Horiba Jobin-Yvon, Munich, Germany) equipped with a 532 nm Nd:YAG laser as described previously (Haider *et al.,* 2010). Raman spectra were baseline corrected and mean normalized in R using the package 'baseline' (Liland and Mevik, Norway) (Lieber and Mahadevan-Jansen, 2003). Machine-learning classification of spectra was performed with the 'randomForest' package (Liaw and Wieners (2002); Merck Research Laboratories, Whitehouse Station, NJ, USA) in R and plotted using non-metric multidimensional scaling.

Protein identification by liquid chromatography and tandem mass spectrometry
Cecal samples were prepared by centrifugation as for FT-IR spectroscopy and microbial pellets were lysed mechanically in the presence of protease inhibitors (Supplementary Methods). After reduction with 10 mM dithiothreitol (10 min, 95 °C) and alkylation with 50 mM iodoacetamide (30 min, room temperature), proteins were separated on 4–12% NuPAGE Bis-Tris gels (Invitrogen, Darmstadt, Germany; cat. no. NP0321BOX) and stained with colloidal Coomassie. The complete protein separation lane of each sample was cut into 12 equal gel pieces (Supplementary Figure S2) and in-gel digestion was performed with sequencing grade trypsin (Promega) (Shevchenko *et al.,* 1996). Peptides were measured using an Eksigent nanoLC-Ultra 1D Plus (Eksigent, Dublin, CA, USA) coupled to a LTQ Orbitrap Velos (Thermo Scientific, Bremen, Germany), as described in detail in the Supplementary Methods.

Metaproteome data analysis
Peak picking and processing of raw MS data was performed as in the Supplementary Methods. To minimize the number of hypothetical proteins, spectra were first searched against a compiled database comprising 81 well-annotated genomes recovered from the Integrated Microbial Genomes website of the Joint Genome Institute (Supplementary Methods). Confounder proteins not expected to be present in the cecal samples were added to the database to ensure specificity. Unmatched spectra were subsequently searched against the entire NCBI database (download date 10/26/2011). For all eight samples (each 12 gel pieces), matched spectra obtained from both database searches were compiled using Scaffold version 3.3.1 (Proteome Software, Portland, OR, USA). Threshold parameters were as follows: protein probability, 95%; minimum number of peptides, 1; peptide probability, 95%. Protein abundances were estimated using NSAF (normalized spectral abundance factor) values calculated from the spectral counts of each individual identified protein (Zybailov *et al.,* 2006). Briefly, in order to account for the fact that larger proteins tend to contribute more peptides or spectra, spectral counts were divided by protein length to provide spectral abundance factors. These factors were normalized against the sum of all spectral abundance factor values in the corresponding run, allowing comparison of protein levels across different runs. NSAF was used as quantitative measure of protein abundances for subsequent statistical analyses. UniProt accession numbers were obtained using the ID mapping function at www.uniprot.org. Protein sequences were downloaded via batch retrieval at the Protein Information Resource website. Protein sequences were assigned to Clusters of Orthologous Groups (COG) by performing a BLASTP (Altschul *et al.,* 1990) against the COG database (Tatusov *et al.,* 2003). BLAST results were further parsed for best hit with an e-value lower than $1e-5$.

High-resolution metabolomics
Cecal samples were prepared by solid-phase extraction as described in the Supplementary Methods.

Ultrahigh resolution mass spectra were acquired using a SOLARIX FT-ICR-MS (Bruker Daltonik GmbH, Bremen, Germany), equipped with a 12 Tesla superconducting magnet and an Apollo II ESI source. FT-ICR-MS settings are given in the Supplementary Methods. Samples were measured in parallel in positive and negative ESI mode due to ionization and detection of different compounds. Raw spectra were processed with Data Analysis Version 4.0 SP2 (Bruker Daltonik GmbH). They were calibrated internally using reference lists of known masses with an error below 0.1 p.p.m. Calibrated spectra were exported to .asc files with a signal-to-noise ratio of 4. The acquired peak lists were aligned by means of in-house software with an error p.p.m. of 1. The aligned data matrix was filtered and only masses detected in at least two of the three biological replicates were kept for subsequent data processing. The filtered matrix was analyzed using Hierarchical Clustering Explorer (College Park, MD, USA) (Seo and Shneiderman, 2002) for unsupervised multivariate data analysis and MultiExperiment Viewer (Saeed *et al.,* 2006) for calculation of significant masses by two-tailed Student's *t*-test (adjusted P-value < 0.01). Possible metabolite identities of significant masses were assigned using the MassTRIX web server (Suhre and Schmitt-Kopplin, 2008) with a maximum error of 1 p.p.m. for both ionization modes. Masses were searched against the KEGG (Kyoto Encyclopedia of Genes and Genomes) (Kanehisa and Goto, 2000), HMDB (Human Metabolome Database) (Wishart *et al.,* 2007) and Lipid Maps (www.lipidmaps.org) databases using *Mus musculus* as reference organism.

Statistics

Unless otherwise stated, statistical tests were done using the R programming environment. For all tests, the bilateral alpha risk was $\alpha = 0.05$. Data were expressed as mean ± s.d. and tested for normal distribution and equality of variances before statistical testing. Non-parametric data were analyzed using the Mann–Whitney U test. The Benjamini–Hochberg procedure was used for multiple testing corrections. For the metaproteomic NSAF data set, the Bioconductor package PLGEM (Power Law Global Error Model) (Pavelka *et al.,* 2004) was used to fit a PLGEM to the NSAF data set. It has been shown that the use of PLGEM-based standard deviations to calculate signal-to-noise ratios in a NSAF data set improves determination of protein expression changes, as it is more conservative with proteins of low abundance than proteins with high abundance. The goodness-of-fit of the model to the NSAF data and the relevant algorithmic details of the PLGEM method are explained in detail elsewhere (Pavelka *et al.,* 2008). Principal component analysis of exported normalized FT-IR spectra was done using SIMCA-P 12.0.1.

Results

High-fat diet induced obesity and altered microbial diversity and composition

The HF diet caused (i) an increase in body weight over the 12-week-long feeding trial (CARB, 29.9 ± 0.63 g; HF, 43.2 ± 4.4 g) (Supplementary Figure S3), (ii) fasting hyperglycemia (Supplementary Table S1) and (iii) a marked reduction in mean cecal mass (tissue plus content): CARB, 342 ± 36 mg; HF, 223 ± 37 mg ($P < 0.001$; *t*-test). To assess the impact of experimental feeding on dominant bacterial communities, we sequenced V4 amplicons of 16S rRNA genes. After trimming, assembly and quality filtering, we obtained a total of 82 698 sequences (6892 ± 2419 per sample) of 233 bp length. The HF diet did not significantly affect taxa richness (Shannon diversity index: CARB, 5.37 ± 0.63; HF 4.96 ± 0.67) (Supplementary Figure S4). *Beta*-diversity analysis (unweighted Unifrac) showed that samples clustered according to diet, although intra-group variations were high (Figure 1a). As expected, phylum-level composition was dominated by members of the *Firmicutes* (71 to 98% of total sequences) and *Bacteroidetes* (1–16%) (Supplementary Table S2). Despite marked inter-individual differences at the family level, sequence proportions were significantly lower for *Ruminococcaceae* (phylum *Firmicutes*) and higher for *Rikenellaceae* (phylum *Bacteroidetes*) in HF mice (Figure 1b and Supplementary Table S3). Lactobacilli were detected in higher proportions in mice fed the HF diet (4–29%), but one control mouse had also a very high proportion (49%). Proportions of *Erysipelotrichales* were higher in three of six HF mice compared with CARB mice, reaching up to 43% in one HF mouse (Supplementary Table S3). The occurrence of 19 dominant operational taxonomic units (OTUs) was significantly affected by the HF diet (Supplementary Table S4). Most of them belonged to the order *Clostridiales* and their sequence numbers were lower in HF mice. In agreement with the aforementioned results, HF mice were characterized by increased numbers of two OTUs within the genus *Alistipes* (a genus in the *Rikenellaceae* with up to 3.5% total sequences). Other major OTUs with a higher prevalence in HF mice included one dominant member of the *Clostridium* cluster XIVa (0.01 vs 4.33% in HF mice) and two *Clostridium* species.

In order to determine if the HF diet causes not only alterations in the composition of the microbiota but also changes to the biochemical environment and microbiota activity in the gut, we performed spectroscopic and mass spectrometric analyses of cecal samples.

Cecal and single-cell chemical fingerprints were diet-specific

To examine the effect of diets on chemical fingerprints in the cecum, samples were analyzed using

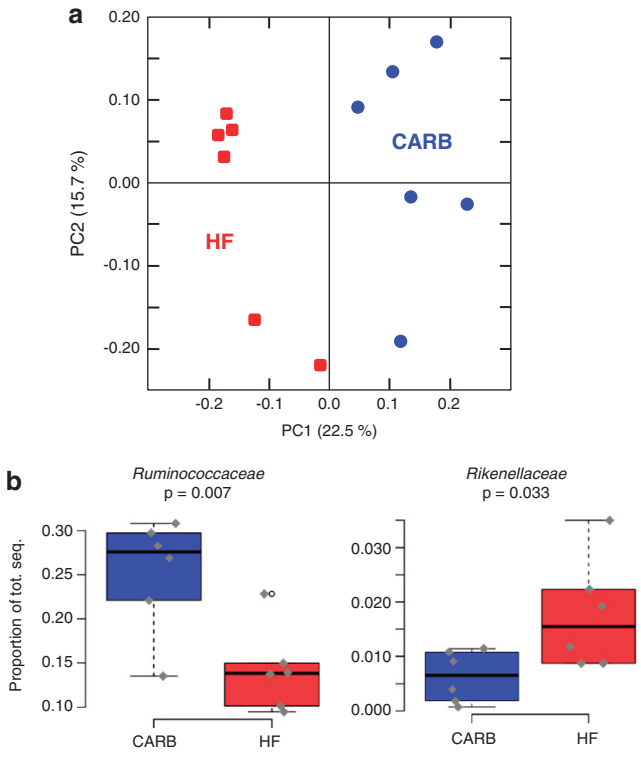

Figure 1 Changes in dominant bacterial diversity and composition. Cecal samples from mice in the CARB and HF group ($n=6$ each) were analyzed by Illumina sequencing of 16S rRNA gene amplicons (V4 region; 233 bp). Sequences were analyzed using QIIME and the RDP. (**a**) Principal component analysis revealed grouping of samples according to diet. (**b**) HF feeding was associated with a significant reduction in the proportion of sequences assigned to the family *Ruminococcaceae* and an increase in the proportion of *Rikenellaceae*. Taxa were assigned using the Greengenes Database (released October 2012).

FT-IR spectroscopy. Cluster analysis of FT-IR spectra revealed a clear separation of chemical fingerprints according to the diet (Figure 2a). There was a clear correlation between peak height and dietary composition in region 2 and 4, which corresponds to lipids and carbohydrates, respectively (Figure 2b). The carbohydrate content was markedly reduced in HF mice, accompanied by a reduced amount of water probably related to reduction in hydration water of carbohydrates and proteins. In spectral region 3 (proteins), the amide I band at 1650 cm^{-1} was clearly reduced in HF samples. In contrast, we observed four new peaks at 1580, 1540 and 1470 as well as one additional peak at 725 cm^{-1}, the absorption of which can be attributed to aromatic rings and heteroaromatic nitro compounds (Colthup *et al.,* 1990). As a proof-of-concept for the impact of bacterial colonization on cecal chemical fingerprints, we compared samples from mice monocolonized with *Bacteroides thetaiotaomicron* to those from conventional mice. As illustrated by microbiota-specific clusters of mice after multivariate analysis, cecal FT-IR spectra were dependent upon the colonization status of mice (Figure 2c). The ability to distinguish altered ecosystem composition on the basis of FT-IR spectra was supported in another mouse cohort by the observation that cecal suspensions after antibiotic treatment clustered distinctly from control samples (cecal preparation from mice on water without antibiotics) (Supplementary Figure S5). However, spectra were overall most affected by the diet, that is, cluster depth after average linkage clustering of samples from conventional mice and gnotobionts on the CARB or HF diet was about threefold higher for diet vs colonization effects (data not shown).

We then aimed at refining the resolution of analysis by comparing the biochemical composition of cecal communities at the level of single cells. Therefore, we used FISH to target members of the abundant groups *Bacteroidales* and *Lachnospiraceae* and measured cellular chemical composition by Raman microspectroscopy. These groups were selected because they were abundant in all mice and alterations in their phylotype composition were observed due to diet. Using fixed cecal biomass from duplicate mice from the CARB and HF group, we acquired a total of 112 single-cell spectra, with 7–20 cells measured for each FISH-defined population in each sample. Analysis with the Random Forests classifier showed that single-cell spectra from Bac-0303 and Erec-0482 groups were clearly distinguishable from each other under both diets (Figure 3a), due in large part to a much higher peak in the Erec-0482 group at 480–482 cm^{-1} (Figure 3b). An effect of the two diets was also observed in the single-cell spectra, especially in the case of Erec-0482-positive cells (Figure 3a). No single peaks alone had high discriminative power for the diet-related differences (Figure 3b), but rather small differences in the intensity of many wave numbers in the spectra collectively allowed for discrimination with the machine-learning classifier.

High-fat diet altered the gut bacterial metaproteome

To corroborate the hypothesis that biochemical changes observed using FT-IR and Raman spectroscopy reflect changes in microbial functions, we further analyzed cecal microbiota from mice fed the CARB and HF diet at the proteome level using LC-MS/MS ($n=4$ mice per diet). The majority of identified proteins (94%) were of bacterial origin. A total of 114 mouse proteins were identified in the samples (Supplementary Results and Supplementary Table S5). After iterative search, 74 553 out of 1 409 370 acquired spectra were matched to 1760 microbial proteins with a false-discovery rate of 0.6% at the protein level (Supplementary Table S5). Of these 1760 proteins, approximately 18% were hypothetical and 29% were housekeeping proteins (ribosomal and chaperone proteins, polymerases, transcription and translation factors). The mean number of spectra and proteins per mouse were as follows: CARB diet,

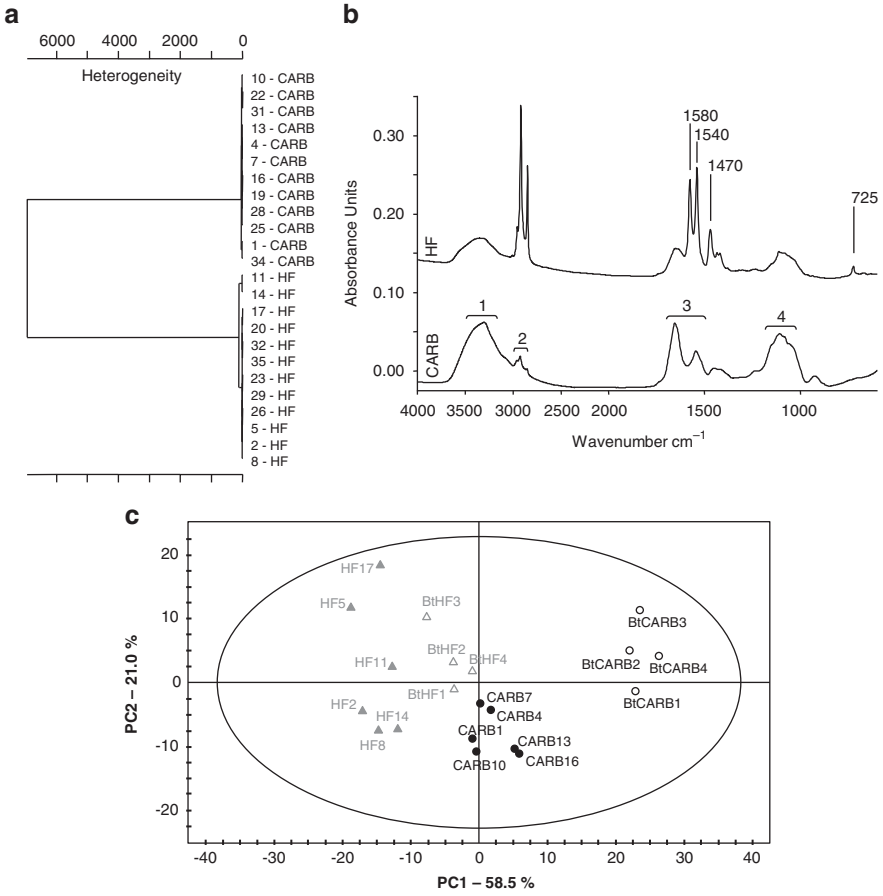

Figure 2 FT-IR-based spectral analysis revealed distinct chemical patterns. (**a**) Cecal microbial pellets from mice fed the same diet clustered together ($n = 12$ mice per diet; trial 1 and 2). Clusters were calculated using the Ward's algorithm and vector normalized first derivatives of the spectra in the range from 3000 to 2800 cm^{-1} and 1800 to 700 cm^{-1}. Mouse ID numbers are shown. Capital letters indicate diets (CARB, carbohydrate; HF, high-fat). (**b**) For each diet, one representative original spectrum is shown. For the sake of clarity, spectra were shifted vertically and the region between 1800 and 700 cm^{-1} was expanded. Regions 1 to 4 depict water-, lipid-, protein- and carbohydrate-specific absorbance wave number ranges, respectively. New peaks arising upon changes in diet are labeled individually. (**c**) Principal component analysis of cecal FT-IR spectra. Input data were spectral intensities from 3000 to 2800 and 1800 to 850 cm^{-1} (598 data points per spectrum). Data were normalized according to integrated spectra (area under the curve) and Pareto scaling. Factor 1 is a projection of mainly lipid (2850 and 2920 cm^{-1}) and protein (1539 and 1576 cm^{-1}) wave numbers. Factor 2 is a projection of mainly carbohydrate (920 to 1080 cm^{-1}) wave numbers. These factors explain 58.5% and 21.0% of the quantitative variations within the wave number span of the spectra, respectively. The mean body weight of mice monocolonized with *B. thetaiotaomicron* was 22.4 ± 1.3 g (CARB) and 26.2 ± 1.9 g (HF) after 3 weeks of experimental feeding ($P = 0.017$; *t*-test). CARB, conventional mice on control diet (black dots); HF, conventional mice on high-fat diet (gray triangles); BtCARB, mice monocolonized with *B. thetaiotaomicron* DSM 2079^T on control diet (circles); BtHF, monocolonized mice on high-fat diet (empty triangles).

$10\,481 \pm 2445$ and 816 ± 68; HF diet, 5377 ± 623 and 579 ± 28. A proportion of 36 and 23% annotated proteins occurred only in CARB and HF mice, respectively (Figure 4a). A heat map including 342 proteins, the occurrence of which was significantly different between the two groups, showed homogenous metaproteome patterns between replicate mice (Figure 4b). After principal component analysis, the two groups of mice clustered very distinctly along PC1, which explained 67% of the variability within the data set (Supplementary Figure S6). For each group, variables (differentially detected proteins) that correlated with PC1 are given in Supplementary Table S5. COG category assignment showed that overall functional patterns were similar in the CARB and HF groups (Supplementary Figure S7) and were dominated by enzymes involved in energy production from carbohydrate metabolism originating from a variety of bacterial species (Supplementary Results and Supplementary Table S5). However, functional assignment of differently detected proteins revealed significant variations between the dietary groups (Figure 4c). The prevalence of functional category C (energy production and conversion), G (carbohydrate metabolism and transport) and O (post-translational modification, protein turnover, chaperone functions) was higher in mice fed the CARB diet whereas the prevalence of category E (amino-acid metabolism and transport), J (translation) and S (unknown functions) was higher in mice fed the HF diet (Supplementary Results and Supplementary Table S5).

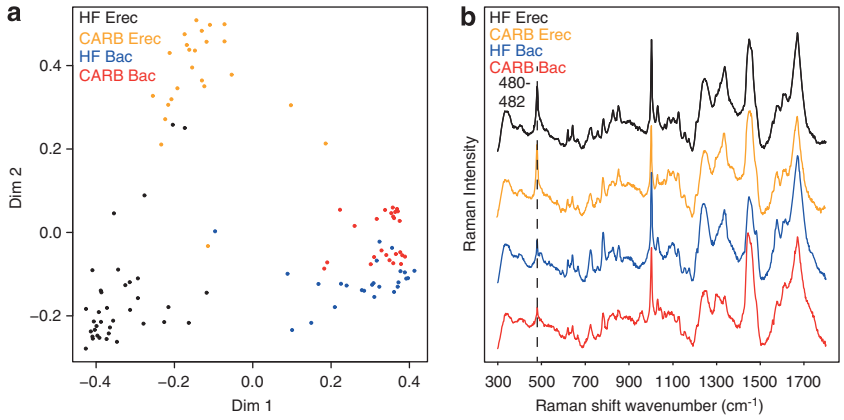

Figure 3 Single-cell characterization of abundant bacterial groups in the cecum by combining FISH and Raman microspectroscopy. Raman spectra were determined for cells from the *Bacteroidales* (identified using probe Bac-0303) and *Lachnospiraceae* (using probe Erec-0482) under high-fat (HF) or carbohydrate (CARB) diet. (**a**) Analysis with the Random Forests classifier revealed clustering of cell spectra by both group and diet on a non-metric multidimensional scaling ordination plot. (**b**) Mean spectra for each bacterial population and dietary group show that the major discriminative peak (480–482 cm^{-1}) is indicative for storage of polyglucan compounds in *Lachnospiraceae*.

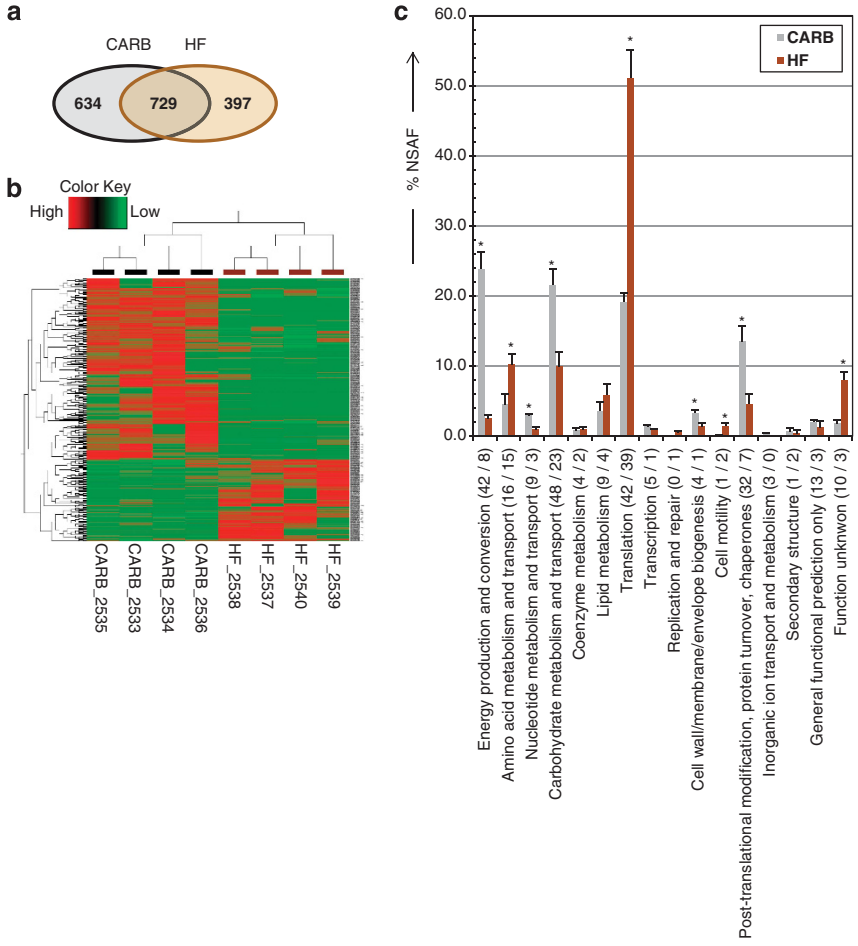

Figure 4 Metaproteome analysis (**a**) Venn diagram showing the occurrence of the 1760 detected microbial proteins. (**b**) Heat map of the 342 differently detected proteins revealed homogenous patterns within each of the two dietary groups. The normalized spectral abundance factors data set was imported into the R programming environment for statistical computing. (**c**) The sequences of dietary group-specific proteins were grouped in COG functional categories by protein BLAST. Categories marked with asterisk were significantly different based on statistical analysis of NSAF proportions ($P<0.01$; two-tailed homoscedastic *t*-test). The number of proteins used for NSAF calculation is given in brackets (CARB/HF) below the *x* axis.

Non-targeted metabolome analysis revealed distinct metabolite patterns

To further describe the cecal ecosystem at the functional level, three cecal contents in each the CARB and HF group were analyzed by FT-ICR-MS to obtain high-resolution metabolite profiles. The complete data set (filtered and significant mass values with annotations) is provided in Supplementary Table S6. The distribution of filtered mass values between the two dietary groups showed that most masses were discriminative (Figure 5a). HF and CARB samples shared only 15 and 28% of features in the negative and positive electrospray ionization mode, respectively, underscoring that diet has a profound impact on cecal biochemical composition and molecular diversity. Cluster analysis resulted in a clear separation of CARB and HF samples, that is, diet-induced effects on the metabolome in cecal contents were much higher than inter-individual differences between the three mice in each group (Figure 5b). A total of 2534 features were significantly different between CARB and HF mice ($P<0.01$). Using MassTRIX annotation and KEGG reference pathways, 86 differently detected metabolites were identified. We noted the presence of fatty acids, steroid hormones, anti-microbial substances (macrolides) and bacterial products such as cis-2-carboxycyclohexyl-acetic acid, cis-2,3-dihydroxy-2,3-dihydro-p-cumate, pravastatin and urobilinogen. Among these metabolites, fatty acids and urobilinogen were specific for the HF diet (Table 2).

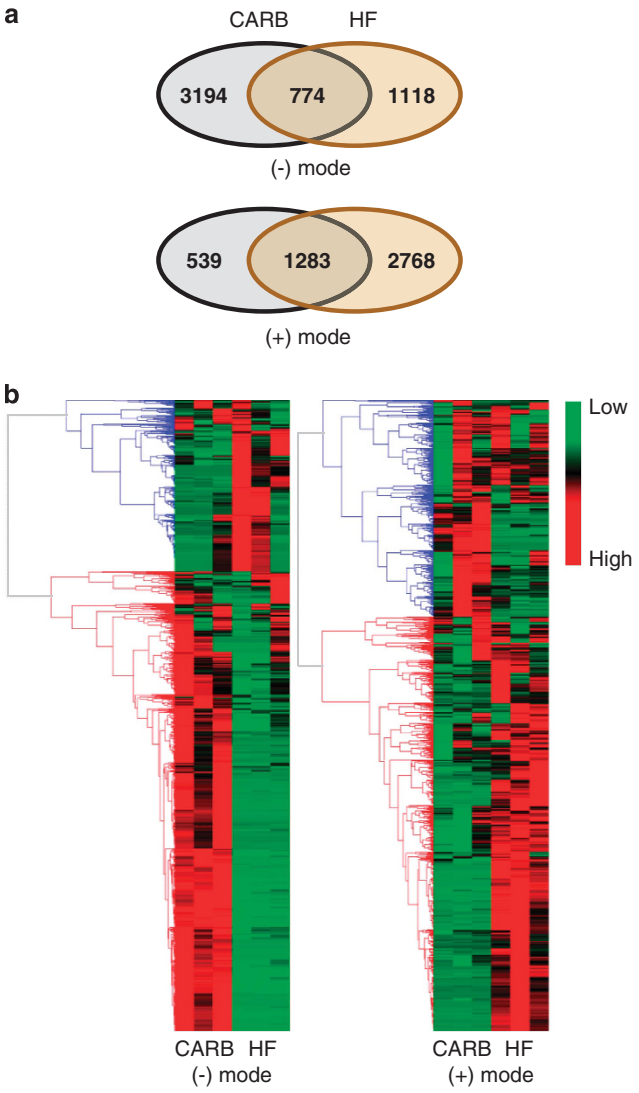

Figure 5 Metabolomic data (**a**) Venn diagrams for positive and negative ESI-FT-ICR-MS mode showing the number of mass values discriminating cecal metabolite patterns from CARB and HF mice (each $n=3$). Most features specific for HF mice and distinguishing the two diets were detected after measurement in positive mode (**b**) Hierarchical cluster analysis using Average Linkage (Unweighted Pair Group Method with Arithmetic Mean) and Pearson correlation coefficient for groups and variables. For each ionization mode, branches within the two main metabolite clusters (*y* axis) appear in blue (e.g. high in CARB in (+) mode) or red (high in HF). Centered and normalized peak intensities are color coded from low (green) to high (red).

Discussion

The intestinal microbiota has been extensively studied at both the phylogenetic and metagenomic level in the context of metabolic disorders. The novelty of the present work lies in the comparative characterization of microbial communities in the mouse cecum at the biochemical level after feeding a HF diet.

We found that HF feeding alters the diversity and composition of intestinal microbiota. Mice in the HF group were characterized by increased relative abundance of *Rikenellaceae*, which is in agreement with other reports based on qPCR and FISH that found no decrease in *Bacteroidetes* following HF feeding (Cani *et al.,* 2008; Duncan *et al.,* 2008). The presence of *Alistipes*, a genus within the *Rikenellaceae*, has also been recently associated with type-2 diabetes in humans (Qin *et al.,* 2012). In addition, we found that *Ruminococcaceae* (phylum *Firmicutes*) were decreased, which makes sense in light of the fact that *ruminococci* are major utilizers of plant polysaccharides, the amount of which is substantially decreased in HF diets (Flint *et al.,* 2012; Ze *et al.,* 2012). Lactic acid bacteria have been proposed to be key players in host metabolic balance (Armougom *et al.,* 2009; Delzenne and Reid, 2009; Arora *et al.,* 2012). Mean *Lactobacillus* relative abundances were generally higher in the HF group (12.5 vs 9.7%), but diet-associated differences were not statistically significant due to marked inter-individual variations. It is worth mentioning that, when compared with studies showing rapid changes in bacterial communities due to high-calorie diets, the data obtained in the present work relate to adaptation of the gut ecosystem and the host to long-term feeding (12 weeks) (Desmarchelier *et al.,* 2012, 2013), which may explain, together with differences in HF diet composition, some of the variations

Table 2 Identified features contributing to diet-specific FT-ICR-MS profiles

	*CARB intensity (*n)	*HF intensity (*n)
CARB diet-specific metabolites		
Steroid hormone biosynthesis		
Allotetra hydrodeoxycorticosterone	6,022,197 (3)	0 (0)
11beta,21-Dihydroxy-5beta-pregnane-3,20-dione[a]	12,256,770 (3)	0 (0)
Aldosterone[b]	40,386,531 (3)	0 (0)
Cortol[c]	19,629,775 (3)	0 (0)
Testosterone glucuronide	3,626,084 (3)	0 (0)
Androsterone glucuronide[d]	16,261,771 (3)	3,900,967 (2)
Microbial metabolism in diverse environments		
cis-2-Carboxycyclohexyl-acetic acid	4,116,462 (3)	0 (0)
cis-2,3-Dihydroxy-2,3-dihydro-p-cumate	2,408,782 (3)	0 (0)
Biosynthesis of 12-, 14-and 16-membered macrolides		
10-Deoxymethynolide	27,444,569 (3)	3,494,241 (2)
8,8a-Deoxyoleandolide	59,777,639 (3)	12,161,516 (3)
Oleandolide	93,629,776 (3)	18,567,187 (3)
6-Deoxyerythronolide B	32,516,089 (3)	3,925,532 (2)
Erythronolide B	63,863,133 (3)	3,720,904 (2)
3-O-alpha-Mycarosylerythronolide B	25,751,484 (3)	0 (0)
Bile acid biosynthesis and bile secretion		
Pravastatin	40,424,347 (3)	9,377,244 (3)
3alpha,7alpha,12alpha,26-Tetra hydroxy-5beta-cholestane	4,727,224 (3)	0 (0)
HF diet-specific metabolites		
Fatty acid biosynthesis		
Decanoic acid	0 (0)	2,509,582 (3)
(6Z,9Z,12Z)-Octadecatrienoic acid[e]	3,648,269 (2)	21,133,473 (3)
(9Z)-Hexadecenoic acid (=palmitoleic acid)	5,110,652 (3)	34,486,283 (3)
Linoleate[f]	4,116,114 (2)	49,977,956 (3)
Tetradeca noic acid (=myristic acid)	6,560,960 (3)	35,976,376 (3)
(8Z,11Z,14Z)-Icosatrienoic acid	7,386,592 (2)	72,601,368 (3)
(9Z)-Octadecenoic acid (=oleic acid)	42,947,039 (3)	1,164,910,976 (3)
Hexadecanoic acid (=palmitic acid)	53,440,799 (3)	856,402,496 (3)
Octadecanoic acid (=stearic acid)	155,914,441 (3)	1,067,133,440 (3)
Porphyrin and chlorophyll metabolism		
D-Urobilinogen[g]	0 (0)	4,375,615 (3)
L-Urobilinogen	1,633,985 (1)	88,861,815 (3)
I-Urobilinogen	31,249,205 (3)	592,250,379 (3)
L-Urobilin	26,692,537 (2)	422,294,496 (3)

FT-ICR-MS, Fourier-transform ion cyclotron resonance mass spectrometry;
Significant masses were annotated using MassTRIX searching against the KEGG, HMDB and Lipid Map databases. Values are mean peak intensities in cecal samples from mice fed the carbohydrate (CARB) or high-fat (HF) diet. Numbers of positive mice are given in brackets.
Superscript letters refer to masses with several possible annotations:
[a]17alpha,21-Dihydroxypregnenolone, 3alpha,21-Dihydroxy-5beta-pregnane-11,20-dione.
[b]Cortisone.
[c]Cortolone.
[d]Etiocholan-3alpha-ol-17-one 3-glucuronide.
[e](9Z,12Z,15Z)-Octadecatrienoic acid, Crepenynate.
[f]9-cis,11-trans-Octadecadienoate.
[g]I-Urobilin.

observed as well as differences with data from the literature (for example, regarding abundance changes of *Bacteroides* or *Erysipelotrichaceae*).

The fact that a HF diet may alter cellular composition of microorganisms is suggested by *in vitro* studies showing that the addition of cholesterol and fatty acids to growth media alter lipid and cell membrane composition of lactic acid bacteria (Dambekodi and Gilliland, 1998; Lye *et al.,* 2010). In the present work, we used FT-IR and Raman spectroscopy to show that a HF diet induces changes in chemical composition of the cecum and single cells as a hint for changes in bacterial physiology. The analysis of cecal samples from mice mono-associated with *B. thetaiotaomicron* vs conventional and from antibiotic-treated mice revealed that, for a given diet, samples clustered distinctly, testifying to the ability to discriminate FT-IR spectra on the basis of microbial community structure. However, spectral distances between diet-dependent clusters were higher than microbiota-driven clusters. Thus, taking into account that the monocolonized, antibiotic-treated and conventional mouse models that we used represent extreme cases, we concluded that diet alters spectra to a higher extent than bacterial composition. It has been shown that the excess of certain nutrients, including lipids, can result in the formation of storage granules

or vesicles in the microbial cells (Bauchart *et al.,* 1990), which can have pronounced effects on FT-IR fingerprints (Naumann, 2000) and may even mask differences in microbial composition (Bosch *et al.,* 2008). Still, it is very likely that part of the spectral differences that we observed were not of microbial origin, that is, due to dietary constituents remaining in the sample or adhering to bacteria. We therefore tested the hypothesis that the differences in diet would result in accumulation of storage compounds by employing single-cell analysis with Raman microspectroscopy. Surprisingly, we found no evidence of increase in storage compounds under either diet, though Erec-0482-positive cells had a higher peak at 480–482 cm^{-1} than Bac-0303-positive cells. This peak is due to intracellular glycogen or polyglucan storage (Movasaghi *et al.,* 2007), which likely reflects the presence of the clostridial-equivalent of glycogen, granulose, a high molecular weight polyglucan important for sporulation (Reysenbach *et al.,* 1986). Nonetheless, analysis of chemical composition at the single-cell level confirmed that the overall cellular composition of bacteria within the abundant bacterial groups *Bacteroidales* and *Lachnospiraceae* was altered by HF feeding, which may be due to the shifting phylotype dynamics that were observed within this group and possibly also altered activity.

While many studies have shown that microbial diversity is altered by dietary changes (Clavel *et al.,* 2005; Martinez *et al.,* 2009; Jumpertz *et al.,* 2011; Kau *et al.,* 2011), much less is known about the impact of diet on the metabolic potential of gut microbiota (Martin *et al.,* 2010; McNulty *et al.,* 2011; Muegge *et al.,* 2011). To our knowledge, this is the first report on the adaptive response of the gut metaproteome to dietary challenge. Since the first gel-based metaproteome published in 2007 (Klaassens *et al.,* 2007) and the state-of-the art LC-MS/MS work by Verberkmoes *et al.* (2009), the size of genomic databases has been rising exponentially. Nevertheless, annotation of peptide spectra remains challenging and functional interpretation based on the occurrence of dominant proteins is limited, that is, taking into account the high degree of diversity of the intestinal microbial ecosystem, we still profit only from a narrow window of analysis at the proteome level (Rooijers *et al.,* 2011; Haange *et al.,* 2012; Kolmeder *et al.*, 2012; Perez-Cobas *et al.,* 2012). This challenge is reflected in the present study by the fact that only 5% of all tandem MS spectra acquired could be matched to protein sequences from the databases. In contrast, up to 50% of all spectra can be commonly identified for sequenced microorganisms.

The total number of proteins identified in the mouse cecal samples that we analyzed ($n = 1760$) is comparable to results obtained using human fecal samples ($n = 1500$ to 1800 proteins) (Verberkmoes *et al.,* 2009; Kolmeder *et al.*, 2012). After functional category assignment of identified proteins, our data confirmed that, regardless of diet, the dominant mammalian gut metaproteome is involved in energy production from carbohydrate metabolism. However, in the HF group, we observed a lower spectra occurrence for proteins classified in COG category C (energy production and conversion). These findings suggest that (i) the microbial ecosystem is not well prepared for efficient energy harvest when 60% of dietary energy originates from fat. The HF diet-induced increase in spectral abundance factors related to category J (translation) may reflect adaptation of microbial cells to meet their needs for survival in a milieu with low energy originating from carbohydrates. For example, *in vitro* studies showed that levels of protein synthesis in marine *Sphingomonas* during starvation were low but preformed ribosomes and whole-cell proteins were retained for at least 7 days in culture (Fegatella and Cavicchioli, 2000). The authors proposed that in starvation, the number of ribosomes is in large excess relative to protein synthesis requirements, which may corroborate increased signals for ribosomal proteins in our HF data sets; and (ii) the depth of analysis (both in terms of biological replicates and protein annotation) is still limiting, that is, only most dominant proteins are detected, which likely prevents better discrimination of the effect of the two diets at the metaproteome level.

Bacterial response to the HF feeding included a sharp decrease in the occurrence of proteins involved in carbohydrate metabolism as well as a reorganization of amino acid metabolism. Indeed, among proteins that best characterized microbiota from mice fed the HF diet, we noted the presence of enzymes metabolizing amino acids (aminotransferases and proteases) that were not detected in CARB mice. We thus propose that shifts in the metabolism of amino acids such as histidine (ammonia-lyase, glutamate formimidoyltransferase, urocanate hydratase) and alanine (alanine and glutamate dehydrogenase) as well as arginine and proline coupled with the use of glutamate as a source of pyruvate for energy production (acetylornithine aminotransferase, glutamate dehydrogenase, (R)-2-hydroxyglutaryl-CoA dehydratase, urease) represent the most prominent metabolic adaptations of the microbial ecosystem to the HF diet (Potrykus *et al.,* 2008). This may corroborate (i) the higher protein to carbohydrate ratio in the HF vs CARB diet (ca. 1:1 vs 1:3), and (ii) increased production of branched-chain fatty acids from the amino acid leucine, isoleucine and valine reported by others after HF feeding in humans or protein fermentation *in vitro* (MacFarlane *et al.,* 1992; Russell *et al.,* 2011). The occurrence of only two of seven enzymes involved in the metabolism of the aforementioned branched-chain amino acids was higher in the HF metaproteome. Of note, in contrast to the suggested increase in the production of short-chain fatty acids linked to higher prevalence of specific members of the *Firmicutes* (for example, *Erysipelotrichaceae*)

in diet-induced obesity (Turnbaugh *et al.,* 2008), evidence from human intervention studies clearly indicates decreased short-chain fatty acids, in particular butyrate, yet increased branched-chain fatty acids concentrations after HF feeding (Brinkworth *et al.,* 2009; Russell *et al.,* 2011). Thus, the notion of increased capacity of the microbiome for energy harvest in the context of diet-induced obesity should be taken with caution, although results may depend on diet composition (for example, content of simple sugars or proteins) and duration of feeding as well as the host phenotype (lean or obese). Most recent metagenomic data suggest that low-diversity (gene count) fecal microbiomes, which seem to be associated with adiposity and metabolic disturbances, are characterized by decreased capability of producing butyrate (Le Chatelier *et al.*, 2013).

The metaproteomic data set is also in agreement with previously published transcriptome analysis and functional prediction of metagenomic sequencing reads (Turnbaugh *et al.,* 2008, 2009). In the aforementioned studies, the authors reported that the cecal metagenome from mice fed a HF/high-sugar Western diet was enriched in genes assigned to glutamate metabolic pathways. They also proposed that the microbiome adapted to the Western diet by increasing transport and conversion of simple sugars and host-derived glycoproteins, which agrees with the higher occurrence of 2-dehydro-3-deoxygluconokinase, 6-phosphofructokinase, *N*-acetylglucosamine-6-phosphate deacetylase and two sugar-binding proteins (gi:282600834 and gi:266619140) in the present HF metaproteomic data set. Also consistent with our results, Yatsunenko *et al.* (2012) recently proposed that a Westernized diet is associated with metagenomes enriched in amino acid- and simple sugar-degrading enzymes when compared with African populations on rural diets high in complex carbohydrates. Finally, the cecal HF metaproteome was characterized by three enzymes (glutaredoxin, alkyl hydroperoxide and thioredoxin reductase) involved in oxidative stress responses, which may reflect adaptation to an environment with altered redox potential (Xiao *et al.,* 2010).

Holmes *et al.* (2012) have provided evidence that the gut microbiome influences host metabolic phenotypes, based primarily on NMR studies (Claus *et al.,* 2008; Calvani *et al.,* 2010). However, only few papers focused on the analysis of metabolites in intestinal content (Martin *et al.,* 2010). In line with the pioneering work by Jansson *et al.*, (2009), we used a non-targeted metabolomic approach based on ultrahigh resolution mass spectrometry to identify diet-derived, host and microbial metabolites in cecal samples. Antunes *et al.* (2011) have also recently used FT-ICR-MS to assess the effect of antibiotics and *Salmonella* infection on the metabolome in mouse feces. They found that both treatments altered host hormone metabolism, for example, production of steroids and eicosanoids. In the present study, we detected prostaglandins, thromboxanes and several steroids and conjugates thereof, which were essentially absent in cecal samples from mice fed the HF diet. This implies that host steroid hormone homeostasis can also be affected by a HF diet. Although literature data are inconsistent, studies have demonstrated that HF diets can influence, for instance, serum testosterone levels in mice and humans (Reed *et al.,* 1987; Meikle *et al.,* 1990; Whyte *et al.,* 2007). Interestingly, the absence of cholesterol-derived products like steroids in the cecum of HF mice corroborates with the finding that mice on the same HF diet were characterized by lower intestinal and hepatic levels of cholesterol in spite of plasma hypercholesterolemia, probably due to increased demand for lipid absorption (Desmarchelier *et al.,* 2012).

Samples from CARB mice were also characterized by the identification of (i) metabolites involved in naphthalene and xylene/cymene degradation by bacteria, and (ii) pravastatin, a potent inhibitor of hydroxymethylglutaryl-CoA reductase with cholesterol-lowering effects, which can also be produced by a variety of bacteria (Serizawa, 1996; Park *et al.,* 2003). In addition, the occurrence of various macrolides in CARB samples may partly explain disturbances in gut microbial composition after HF feeding due to changes in the pool of anti-microbial substances present in the cecum. In cecal samples from mice fed the HF diet, fatty acid levels were much higher than in CARB mice, reflecting the proportion of major fatty acids in the HF diet (12% oleic acid, 8% palmitic acid, 6% stearic acid, 2% linoleic acid). We also noted the presence of a ceramide (*N*-acylsphingosine), for which *de novo* synthesis may be promoted by high levels of palmitate in the HF diet. Ceramide production may also be enhanced by hydrolysis of sphingomyelin, which corroborates with the detection of a secreted protein of the sphingomyelinase family (sp|P58242|ASM3B_MOUSE) in the mouse cecal proteome after HF feeding. Of note, ceramides have been implicated in diet-induced insulin resistance (Longato *et al.,* 2011) and have cytotoxic and pro-apoptotic properties (Haimovitz-Friedman *et al.,* 1997; Jarvis and Grant, 1998). Finally, the conversion of bilirubin to urobilinogen is considered to be a specific feature of the gut microbiota, especially *Clostridium* spp. (Becker *et al.,* 2011). Thus, higher levels of urobilinogen and its oxidized product urobilin in the cecum of HF mice (i) testify to diet-induced functional alterations of the microbial ecosystem, (ii) may be related to the observed HF-induced increase in phylotypes within the *Clostridiales*, an order that includes known converters of bilirubin, and (iii) could explain the appearance of the FT-IR spectral features attributed to aromatic and heteroaromatic ring vibrations in the cecum of HF mice. Due to the relatively limited number of samples analyzed and to the fact that data sets were obtained from different mice and that a minor

fraction of metabolite masses can be annotated, we did not integrate data and extrapolate on functional links between the metaproteome and metabolome.

In summary, we demonstrated that (i) diet can alter the biochemical composition of the gut microbiota either by shifting phylotype composition or the activity of bacterial cells, (ii) changes in bacterial metaproteome after HF feeding are most pronounced for pathways of amino acid metabolism, and (iii) cecal metabolic pathways affected by HF feeding include eicosanoid, steroid hormone, macrolide, bile acid and bilirubin metabolism. These findings show that a HF diet has a major impact on the mouse cecal microbiota that extends beyond compositional changes to major alterations in bacterial physiology and metabolite landscape. Molecular mechanisms underlying the conversion of steroids and amino acids by specific gut bacteria in relation with the onset of metabolic disorders appear to be of particular relevance for future targeted experimental work.

Acknowledgements

Raw files obtained by metaproteomic and metabolomic spectrometry measurements are available upon request. We thank Adelmar Stamfort and Pia Baur for helping with statistical analysis, Nico Gebhardt, Ines Grüner, Elmar Jocham, Melanie Klein, Ute Lehmann, Ronny Scheundel and Caroline Ziegler for technical assistance, and Gabriele Hörmannsperger for reviewing the manuscript. Charles Desmarchelier was financed by the EU FP6 project *Nutrient Sensing in Satiety Control and Obesity* (NuSISCO, grant no. MEST-CT-2005-020494). Chrisoph Böhm, David Berry, and Michael Wagner were supported by the European Research Council (Advanced Grant NITRICARE 294343) and David Berry was supported by the Vienna Science and Technology Fund (WWTF) through project LS12-001.

References

Altschul SF, Gish W, Miller W, Myers EW, Lipman DJ. (1990). Basic local alignment search tool. *J Mol Biol* **215**: 403–410.

Antunes LC, Arena ET, Menendez A, Han J, Ferreira RB, Buckner MM *et al.* (2011). Impact of salmonella infection on host hormone metabolism revealed by metabolomics. *Infect Immun* **79**: 1759–1769.

Antunes LC, Han J, Ferreira RB, Lolic P, Borchers CH, Finlay BB. (2011). Effect of antibiotic treatment on the intestinal metabolome. *Antimicrob Agents Chemother* **55**: 1494–1503.

Armougom F, Henry M, Vialettes B, Raccah D, Raoult D. (2009). Monitoring bacterial community of human gut microbiota reveals an increase in Lactobacillus in obese patients and Methanogens in anorexic patients. *PLoS One* **4**: e7125.

Arora T, Anastasovska J, Gibson G, Tuohy K, Sharma RK, Bell J *et al.* (2012). Effect of *Lactobacillus acidophilus* NCDC 13 supplementation on the progression of obesity in diet-induced obese mice. *Br J Nutr* **108**: 1382–1389.

Backhed F, Ding H, Wang T, Hooper LV, Koh GY, Nagy A *et al.* (2004). The gut microbiota as an environmental factor that regulates fat storage. *Proc Natl Acad Sci USA* **101**: 15718–15723.

Bauchart D, Legay-Carmier F, Doreau M, Gaillard B. (1990). Lipid metabolism of liquid-associated and solid-adherent bacteria in rumen contents of dairy cows offered lipid-supplemented diets. *Br J Nutr* **63**: 563–578.

Becker N, Kunath J, Loh G, Blaut M. (2011). Human intestinal microbiota: characterization of a simplified and stable gnotobiotic rat model. *Gut Microbes* **2**: 25–33.

Berry D, Schwab C, Milinovich G, Reichert J, Ben Mahfoudh K, Decker T *et al.* (2012). Phylotype-level 16S rRNA analysis reveals new bacterial indicators of health state in acute murine colitis. *ISME J* **6**: 2091–2106.

Blaut M, Clavel T. (2007). Metabolic diversity of the intestinal microbiota: implications for health and disease. *J Nutr* **137**: 751S–755S.

Bosch A, Minan A, Vescina C, Degrossi J, Gatti B, Montanaro P *et al.* (2008). Fourier transform infrared spectroscopy for rapid identification of nonfermenting gram-negative bacteria isolated from sputum samples from cystic fibrosis patients. *J Clin Microbiol* **46**: 2535–2546.

Brinkworth GD, Noakes M, Clifton PM, Bird AR. (2009). Comparative effects of very low-carbohydrate, high-fat and high-carbohydrate, low-fat weight-loss diets on bowel habit and faecal short-chain fatty acids and bacterial populations. *Br J Nutr* **101**: 1493–1502.

Calvani R, Miccheli A, Capuani G, Tomassini Miccheli A, Puccetti C, Delfini M *et al.* (2010). Gut microbiome-derived metabolites characterize a peculiar obese urinary metabotype. *Int J Obes (Lond)* **34**: 1095–1098.

Cani PD, Bibiloni R, Knauf C, Waget A, Neyrinck AM, Delzenne NM *et al.* (2008). Changes in gut microbiota control metabolic endotoxemia-induced inflammation in high-fat diet-induced obesity and diabetes in mice. *Diabetes* **57**: 1470–1481.

Caporaso JG, Kuczynski J, Stombaugh J, Bittinger K, Bushman FD, Costello EK *et al.* (2010). QIIME allows analysis of high-throughput community sequencing data. *Nat Methods* **7**: 335–336.

Claus SP, Tsang TM, Wang Y, Cloarec O, Skordi E, Martin FP *et al.* (2008). Systemic multicompartmental effects of the gut microbiome on mouse metabolic phenotypes. *Mol Syst Biol* **4**: 219.

Clavel T, Fallani M, Lepage P, Levenez F, Mathey J, Rochet V *et al.* (2005). Isoflavones and functional foods alter the dominant intestinal microbiota in postmenopausal women. *J Nutr* **135**: 2786–2792.

Cole JR, Chai B, Marsh TL, Farris RJ, Wang Q, Kulam SA *et al.* (2003). The Ribosomal Database Project (RDP-II): previewing a new autoaligner that allows regular updates and the new prokaryotic taxonomy. *Nucleic Acids Res* **31**: 442–443.

Colthup NB, Daly LH, Wiberley SE. (1990). *Introduction to Infrared and Raman Spectroscopy*, 3rd edn Academic Press: Boston.

Dambekodi PC, Gilliland SE. (1998). Incorporation of cholesterol into the cellular membrane of Bifidobacterium longum. *J Dairy Sci* **81**: 1818–1824.

Delzenne N, Reid G. (2009). No causal link between obesity and probiotics. *Nat Rev Microbiol* **7**: 901, author reply 901.

Delzenne NM, Cani PD. (2011). Interaction between obesity and the gut microbiota: relevance in nutrition. *Annu Rev Nutr* **31**: 15–31.

Desmarchelier C, Dahlhoff C, Keller S, Sailer M, Jahreis G, Daniel H. (2012). C57Bl/6 N mice on a western diet display reduced intestinal and hepatic cholesterol levels despite a plasma hypercholesterolemia. *BMC Genomics* **13**: 84.

Desmarchelier C, Ludwig T, Scheundel R, Rink N, Bader BL, Klingenspor M *et al.* (2013). Diet-induced obesity in *ad libitum*-fed mice: food texture overrides the effect of macronutrient composition. *Br J Nutr* **109**: 1518–1527.

Duncan SH, Lobley GE, Holtrop G, Ince J, Johnstone AM, Louis P *et al.* (2008). Human colonic microbiota associated with diet, obesity and weight loss. *Int J Obes (Lond)* **32**: 1720–1724.

Fegatella F, Cavicchioli R. (2000). Physiological responses to starvation in the marine oligotrophic *ultramicrobacterium Sphingomonas* sp. strain RB2256. *Appl Environ Microbiol* **66**: 2037–2044.

Fleissner CK, Huebel N, Abd El-Bary MM, Loh G, Klaus S, Blaut M. (2010). Absence of intestinal microbiota does not protect mice from diet-induced obesity. *Br J Nutr* **104**: 919–929.

Flint HJ, Scott KP, Duncan SH, Louis P, Forano E. (2012). Microbial degradation of complex carbohydrates in the gut. *Gut Microbes* **3**: 289–306.

Franks AH, Harmsen HJ, Raangs GC, Jansen GJ, Schut F, Welling GW. (1998). Variations of bacterial populations in human feces measured by fluorescent in situ hybridization with group-specific 16S rRNA-targeted oligonucleotide probes. *Appl Environ Microbiol* **64**: 3336–3345.

Haange SB, Oberbach A, Schlichting N, Hugenholtz F, Smidt H, von Bergen M *et al.* (2012). Metaproteome analysis and molecular genetics of rat intestinal microbiota reveals section and localization resolved species distribution and enzymatic functionalities. *J Proteome Res* **11**: 5406–5417.

Haider S, Wagner M, Schmid MC, Sixt BS, Christian JG, Hacker G *et al.* (2010). Raman microspectroscopy reveals long-term extracellular activity of Chlamydiae. *Mol Microbiol* **77**: 687–700.

Haimovitz-Friedman A, Cordon-Cardo C, Bayoumy S, Garzotto M, McLoughlin M, Gallily R *et al.* (1997). Lipopolysaccharide induces disseminated endothelial apoptosis requiring ceramide generation. *J Exp Med* **186**: 1831–1841.

Heymsfield SB, Pietrobelli A. (2011). Individual differences in apparent energy digestibility are larger than generally recognized. *Am J Clin Nutr* **94**: 1650–1651.

Holmes E, Li JV, Marchesi JR, Nicholson JK. (2012). Gut microbiota composition and activity in relation to host metabolic phenotype and disease risk. *Cell Metab* **16**: 559–564.

Huang WE, Stoecker K, Griffiths R, Newbold L, Daims H, Whiteley AS *et al.* (2007). Raman-FISH: combining stable-isotope Raman spectroscopy and fluorescence *in situ* hybridization for the single cell analysis of identity and function. *Environ Microbiol* **9**: 1878–1889.

Hörmannsperger G, Clavel T, Haller D. (2012). Gut matters: microbe-host interactions in allergic diseases. *J Allergy Clin Immunol* **129**: 1452–1459.

Jansson J, Willing B, Lucio M, Fekete A, Dicksved J, Halfvarson J *et al.* (2009). Metabolomics reveals metabolic biomarkers of Crohn's disease. *PLoS One* **4**: e6386.

Jarvis WD, Grant S. (1998). The role of ceramide in the cellular response to cytotoxic agents. *Curr Opin Oncol* **10**: 552–559.

Jumpertz R, Le DS, Turnbaugh PJ, Trinidad C, Bogardus C, Gordon JI *et al.* (2011). Energy-balance studies reveal associations between gut microbes, caloric load, and nutrient absorption in humans. *Am J Clin Nutr* **94**: 58–65.

Kanehisa M, Goto S. (2000). KEGG: kyoto encyclopedia of genes and genomes. *Nucleic Acids Res* **28**: 27–30.

Kau AL, Ahern PP, Griffin NW, Goodman AL, Gordon JI. (2011). Human nutrition, the gut microbiome and the immune system. *Nature* **474**: 327–336.

Klaassens ES, de Vos WM, Vaughan EE. (2007). Metaproteomics approach to study the functionality of the microbiota in the human infant gastrointestinal tract. *Appl Environ Microbiol* **73**: 1388–1392.

Kolmeder CA, de Been M, Nikkila J, Ritamo I, Matto J, Valmu L *et al.* (2012). Comparative metaproteomics and diversity analysis of human intestinal microbiota testifies for its temporal stability and expression of core functions. *PLoS One* **7**: e29913.

Le Chatelier E, Nielsen T, Qin J, Prifti E, Hildebrand F, Falony G *et al.* (2013). Richness of human gut microbiome correlates with metabolic markers. *Nature* **500**: 541–546.

Lepage P, Leclerc MC, Joossens M, Mondot S, Blottiere HM, Raes J *et al.* (2013). A metagenomic insight into our gut's microbiome. *Gut* **62**: 146–158.

Liaw A, Wiener M. (2002). Classification and Regression by randomForest. *R News* **2**: 18–22.

Lieber CA, Mahadevan-Jansen A. (2003). Automated method for subtraction of fluorescence from biological Raman spectra. *Appl Spectrosc* **57**: 1363–1367.

Longato L, Tong M, Wands JR, de la Monte SM. (2011). High fat diet induced hepatic steatosis and insulin resistance: Role of dysregulated ceramide metabolism. *Hepatol Res* **42**: 412–427.

Lye HS, Rusul G, Liong MT. (2010). Removal of cholesterol by lactobacilli via incorporation and conversion to coprostanol. *J Dairy Sci* **93**: 1383–1392.

MacFarlane GT, Gibson G, Beatty E, Cummings JH. (1992). Estimation of short-chain fatty acid production from protein by human intestinal bacteria based on branched-chain fatty acid measurments. *FEMS Microbiol Ecol* **101**: 81–88.

Manz W, Amann R, Ludwig W, Vancanneyt M, Schleifer KH. (1996). Application of a suite of 16S rRNA-specific oligonucleotide probes designed to investigate bacteria of the phylum Cytophaga-Flavobacter-Bacteroides in the natural environment. *Microbiology* **142**: 1097–1106.

Martin FP, Sprenger N, Montoliu I, Rezzi S, Kochhar S, Nicholson JK. (2010). Dietary modulation of gut functional ecology studied by fecal metabonomics. *J Proteome Res* **9**: 5284–5295.

Martinez I, Wallace G, Zhang C, Legge R, Benson AK, Carr TP *et al.* (2009). Diet-induced metabolic improvements in a hamster model of hypercholesterolemia are strongly linked to alterations of the gut microbiota. *Appl Environ Microbiol* **75**: 4175–4184.

Masella AP, Bartram AK, Truszkowski JM, Brown DG, Neufeld JD. (2012). PANDAseq: paired-end assembler for illumina sequences. *BMC Bioinformatics* **13**: 31.

McNulty NP, Yatsunenko T, Hsiao A, Faith JJ, Muegge BD, Goodman AL *et al.* (2011). The impact of a consortium

of fermented milk strains on the gut microbiome of gnotobiotic mice and monozygotic twins. *Sci Transl Med* **3**: 106ra106.

Meikle AW, Stringham JD, Woodward MG, McMurry MP. (1990). Effects of a fat-containing meal on sex hormones in men. *Metabolism* **39**: 943–946.

Movasaghi Z, Rehman S, Rehman I. (2007). Raman spectroscopy of biological tissues. *Appl Spectrosc Rev* **42**: 493–541.

Muegge BD, Kuczynski J, Knights D, Clemente JC, Gonzalez A, Fontana L *et al.* (2011). Diet drives convergence in gut microbiome functions across mammalian phylogeny and within humans. *Science* **332**: 970–974.

Naumann D. (2000). *Infrared Spectroscopy in Microbiology* In Encyclopedia of analytical chemistry. In RA Meyers (ed.) John Wiley & Sons: Chichester; pp 102–131.

Park JW, Lee JK, Kwon TJ, Yi DH, Kim YJ, Moon SH *et al.* (2003). Bioconversion of compactin into pravastatin by *Streptomyces* sp. *Biotechnol Lett* **25**: 1827–1831.

Patel RK, Jain M. (2012). NGS QC Toolkit: a toolkit for quality control of next generation sequencing data. *PLoS One* **7**: e30619.

Pavelka N, Fournier ML, Swanson SK, Pelizzola M, Ricciardi-Castagnoli P, Florens L *et al.* (2008). Statistical similarities between transcriptomics and quantitative shotgun proteomics data. *Mol Cell Proteomics* **7**: 631–644.

Pavelka N, Pelizzola M, Vizzardelli C, Capozzoli M, Splendiani A, Granucci F *et al.* (2004). A power law global error model for the identification of differentially expressed genes in microarray data. *BMC Bioinformatics* **5**: 203.

Perez-Cobas AE, Gosalbes MJ, Friedrichs A, Knecht H, Artacho A, Eismann K *et al.* (2012). Gut microbiota disturbance during antibiotic therapy: a multi-omic approach. *Gut;* doi:10.1136/gutjnl-2012-303184.

Potrykus J, White RL, Bearne SL. (2008). Proteomic investigation of amino acid catabolism in the indigenous gut anaerobe *Fusobacterium varium*. *Proteomics* **8**: 2691–2703.

Qin J, Li Y, Cai Z, Li S, Zhu J, Zhang F *et al.* (2012). A metagenome-wide association study of gut microbiota in type 2 diabetes. *Nature* **490**: 55–60.

Raoult D, Fournier PE, Drancourt M. (2004). What does the future hold for clinical microbiology? *Nat Rev Microbiol* **2**: 151–159.

Reed MJ, Cheng RW, Simmonds M, Richmond W, James VH. (1987). Dietary lipids: an additional regulator of plasma levels of sex hormone binding globulin. *J Clin Endocrinol Metab* **64**: 1083–1085.

Reysenbach AL, Ravenscroft N, Long S, Jones DT, Woods DR. (1986). Characterization, biosynthesis, and regulation of granulose in *clostridium acetobutylicum*. *Appl Environ Microbiol* **52**: 185–190.

Rooijers K, Kolmeder C, Juste C, Dore J, de Been M, Boeren S *et al.* (2011). An iterative workflow for mining the human intestinal metaproteome. *BMC Genomics* **12**: 6.

Russell WR, Gratz SW, Duncan SH, Holtrop G, Ince J, Scobbie L *et al.* (2011). High-protein, reduced-carbohydrate weight-loss diets promote metabolite profiles likely to be detrimental to colonic health. *Am J Clin Nutr* **93**: 1062–1072.

Saeed A, Bhagabati N, Braisted J, Liang W, Sharov V, Howe E *et al.* (2006). TM4 microarray software suite. DNA microarrays, part B: databases and statistics. *A. Kimmel and B. Oliver*. Elsevier Academic Press: San Diego, Vol. **411:** 134–193.

Seo J, Shneiderman B. (2002). Interactively exploring hierarchical clustering results. *IEEE Computer* **35**: 80–86.

Serizawa N. (1996). Biochemical and molecular approaches for production of pravastatin, a potent cholesterol-lowering drug. *Biotechnol Annu Rev* **2**: 373–389.

Shevchenko A, Wilm M, Vorm O, Mann M. (1996). Mass spectrometric sequencing of proteins silver-stained polyacrylamide gels. *Anal Chem* **68**: 850–858.

Suhre K, Schmitt-Kopplin P. (2008). MassTRIX: mass translator into pathways. *Nucleic Acids Res* **36**: W481–W484.

Tatusov RL, Fedorova ND, Jackson JD, Jacobs AR, Kiryutin B, Koonin EV *et al.* (2003). The COG database: an updated version includes eukaryotes. *BMC Bioinformatics* **4**: 41.

Turnbaugh P, Ridaura V, Faith J, Rey F, Knight R, Gordon J. (2009). The effect of diet on the human gut microbiome: a metagenomic analysis in humanized gnotobiotic mice. *Sci Transl Med* **1**: 6ra14.

Turnbaugh PJ, Backhed F, Fulton L, Gordon JI. (2008). Diet-induced obesity is linked to marked but reversible alterations in the mouse distal gut microbiome. *Cell Host Microbe* **3**: 213–223.

Turnbaugh PJ, Ley RE, Mahowald MA, Magrini V, Mardis ER, Gordon JI. (2006). An obesity-associated gut microbiome with increased capacity for energy harvest. *Nature* **444**: 1027–1031.

Verberkmoes NC, Russell AL, Shah M, Godzik A, Rosenquist M, Halfvarson J *et al.* (2009). Shotgun metaproteomics of the human distal gut microbiota. *Isme J* **3**: 179–189.

Wenning M, Theilmann V, Scherer S. (2006). Rapid analysis of two food-borne microbial communities at the species level by Fourier-transform infrared microspectroscopy. *Environ Microbiol* **8**: 848–857.

Whyte JJ, Alexenko AP, Davis AM, Ellersieck MR, Fountain ED, Rosenfeld CS. (2007). Maternal diet composition alters serum steroid and free fatty acid concentrations and vaginal pH in mice. *J Endocrinol* **192**: 75–81.

Wishart DS, Tzur D, Knox C, Eisner R, Guo AC, Young N *et al.* (2007). HMDB: the Human Metabolome Database. *Nucleic Acids Res* **35**: D521–D526.

Xiao Y, Cui J, Shi YH, Sun J, Wang ZP, Le GW. (2010). Effects of duodenal redox status on calcium absorption and related genes expression in high-fat diet-fed mice. *Nutrition* **26**: 1188–1194.

Yatsunenko T, Rey FE, Manary MJ, Trehan I, Dominguez-Bello MG, Contreras M *et al.* (2012). Human gut microbiome viewed across age and geography. *Nature* **486**: 222–227.

Ze X, Duncan SH, Louis P, Flint HJ. (2012). Ruminococcus bromii is a keystone species for the degradation of resistant starch in the human colon. *ISME J* **6**: 1535–1543.

Zybailov B, Mosley AL, Sardiu ME, Coleman MK, Florens L, Washburn MP. (2006). Statistical analysis of membrane proteome expression changes in Saccharomyces cerevisiae. *J Prot Res* **5**: 2339–2347.

Supplementary Information accompanies this paper on The ISME Journal website (http://www.nature.com/ismej)